

Water transport throughout the TRAPPIST-1 system: the role of planetesimals

Vladimir Došović,¹★ Bojan Novaković,¹ Branislav Vukotić,² Milan M. Ćirković²

¹*Department of Astronomy, Faculty of Mathematics, University of Belgrade, Studentski Trg 16, 11000 Belgrade, Serbia*

²*Astronomical Observatory of Belgrade, Volgina 7, 11000 Belgrade, Serbia*

Accepted XXX. Received YYY; in original form ZZZ

ABSTRACT

Observational data suggest that a belt of planetesimals is expected close to the snow line in protoplanetary disks. Assuming there is such a belt in TRAPPIST-1 system, we examine possibilities of water delivery to the planets via planetesimals from the belt. The study is accomplished by numerical simulations of dynamical evolution of a hypothetical planetesimal belt. Our results show that the inner part of the belt is dynamically unstable and planetesimals located in this region are quickly scattered away, with many of them entering the region around the planets. The main dynamical mechanism responsible for the instability are close encounters with the outermost planet Trappist-1h. A low-order mean-motion resonance 2:3 with Trappist-1h, located in the same region, also contributes to the objects transport. In our nominal model, the planets have received non-negligible amount of water, with the smallest amount of 15% of the current Earth’s water amount (EWA) being delivered to the planet 1b, while the planets Trappist-1e and Trappist-1g have received more than 60% of the EWA. We have found that while the estimated efficiency of water transport to the planets is robust, the amount of water delivered to each planet may vary significantly depending on the initial masses and orbits of the planets. The estimated dynamical „half-lives” have shown that the impactors’ source region should be emptied in less than 1 Myr. Therefore, the obtained results suggest that transport of planetesimals through the system preferably occurs during an early phase of the planetary system evolution.

Key words: Planetary systems – planets and satellites: individual: TRAPPIST-1 – planets and satellites: dynamical evolution and stability – celestial mechanics – astrobiology – methods: numerical

1 INTRODUCTION

The TRAPPIST-1 system was discovered in 2016, using TRAnsiting Planets and PlanetesImals Small Telescope (Gillon et al. 2016). The system is around 12 pc away from the Earth, and consists of seven Earth-like planets (Gillon et al. 2017). Even though TRAPPIST-1 is a very old system, aged 7.6 ± 2.2 Gyr (Burgasser & Mamajek 2017), it is a very compact system, with all the planets orbiting within 0.07 au. Stability of this compact system is explained by a resonant chain that possibly includes all seven planets (Tamayo et al. 2017; Luger et al. 2017).

Habitable Zone (HZ), when considered in the context of planetary science, is an area around host star where temperature allows liquid water to exist on planetary surface (Gonzalez 2005). From anthropocentric viewpoint, the ex-

istence of liquid water at planetary surface at fairly wide range of atmospheric compositions and pressures is required for growth and development of life. For this reason, it is important to determine whether or not there is a liquid water on at least some of the planets in TRAPPIST-1 system, or at least whether there could have been significant amounts of it in the past. The case of Mars, which is often regarded as fully habitable during the early Noachian age and perhaps marginally habitable today, shows that even water locked in subsurface deposits or permafrost counts toward the habitability index (Westall et al. 2015).

Water could be incorporated in planets during their formation or be delivered at later stages of planetary system evolution. Since the planets located inside habitable zones are likely formed inside a snow line, and thus are not made of water-rich materials (Fritz et al. 2014; Ida, Yamamura, & Okuzumi 2019), water at their surfaces could have been transported from outer parts of a plan-

★ E-mail: vladimir_djosovic@matf.bg.ac.rs

etary system. For a long time only postulated, the existence of such water reservoirs in the outer regions of planetary systems in the course of their formation has been also observationally confirmed (e.g. Hogerheijde, et al. 2011; Kama, et al. 2016). In this case, water could be reimbursed at subsequent stages of evolution of the planetary systems, during their migration stages (Tsiganis, et al. 2005; Unterborn et al. 2018). On the other hand, some papers (Coleman, et al. 2017, 2019; Schoonenberg, et al. 2019) suggested that planets would form outside of snow line, and then migrate inward, thus accumulating higher water fractions. However, in the latter scenario, the water on some TRAPPIST-1 planets would likely be lost due to an XUV emission from Ultra Cold Dwarf star (Bolmont et al. 2017) through whole lifetime of planetary system. Still, water on them could be delivered after disk phase, at even later stages of evolution of the planetary system, during impacts of planetesimals originating outside of the snow line, thus containing volatile materials (Kral et al. 2018; Cuntz, Loibnegger & Dvorak 2018).

For the planets in TRAPPIST-1 system, especially for those located inside the habitable zone, it is important to estimate the origin and amount of their water content. Papaloizou, Szuszkiewicz, & Terquem (2018) found that three out of the seven planets in this system, namely Trappist-1e, Trappist-1f, and Trappist-1g, are in the host star habitable zone. Additional analyses of the tidal heating (Dobos, Barr & Kiss 2019), and climate modeling for planets in TRAPPIST-1 (Lincowski et al. 2018), suggest that the most habitable planet in this system should be Trappist-1e.

The first indication of the existence of water at the surfaces of planets Trappist-1b and Trappist-1c, comes from the Hubble Space Telescope observations (de Wit et al. 2016). Moreover, using numerical simulation of transit timing variations, Grimm et al. (2018) successfully determine densities of the planets in TRAPPIST-1 system, and therefore planetary masses as well. Furthermore, based on these results, and known diameters of the planets obtained by transit method (Gillon et al. 2016, 2017), Grimm et al. (2018) also estimated composition of each of the planets. They suggested that the planets Trappist-1c and Trappist-1e are almost completely rocky, while on Trappist-1b, 1d, 1f, and 1g, the existence of a surface envelope is possible, either in a form of water-ice, ocean or an atmosphere.

It is well known that objects with about a kilometer in diameter are residuals of planet formation (Goldreich, Lithwick, & Sari 2004), regardless of the mechanism of their creation. The existence of planetesimal belt similar to the one in Solar System is confirmed observationally in some other planetary systems as well (van der Marel et al. 2013). Such objects could have high influence on their neighborhood in many different ways, including transport of materials from one part of the system to another. A well-known example is the transport of water in our Solar System (O'Brien et al. 2014), but a similar approach has been applied also to other planetary systems (Dvorak, Loibnegger & Cuntz 2020; Frantseva et al. 2020).

Many small objects in the inner Solar System are known to contain some amount of water. The largest object in asteroid belt, (1) Ceres, likely contains at least 20%-30% water by mass (McCord & Sotin 2005; Castillo-Rogez & McCord 2010; Thangjam et al. 2018). The water-ice has been de-

tected at the surface of asteroid (24) Themis (Campins et al. 2010; Rivkin & Emery 2010), while the so-called main-belt comets (MBCs), a subgroup of active asteroids, are expected to contain significant amount of water (Jewitt 2012; Snodgrass et al. 2017). The association of MBCs to primitive collisional asteroid families implies that water-ice is almost everywhere in the asteroid belt (Hsieh, et al. 2018). Finally, recent result from the NASA's OSIRIS-REx mission suggests that hydrated minerals are widespread on near-Earth asteroid (101955) Bennu (Hamilton, et al. 2019). Although this does not imply that Bennu contains any water right now, it shows that its parent body, probably a larger asteroid than Bennu, did contain water. These facts show that water could be widespread even among the objects in asteroid-like extrasolar planetesimal belts.

A possibility to replenish planetary water reservoirs in TRAPPIST-1 system via impacts by water-rich planetesimals was a subject of two recent studies. A water transport from the outer part of TRAPPIST-1 system was studied by Kral et al. (2018). These authors assumed existence of planetesimals on cometary-like eccentric orbits in the system, and analyzed a potential effect of these objects for water delivery and formation of the secondary atmospheres. They showed that significant amount of water could be transported in such a way and that the secondary atmospheres could be formed. The eccentric orbits however are not a natural outcome of planetesimal formation process (Yang, Mac Low, & Menou 2009), but may be produced during a subsequent dynamical evolution. Still, such dynamical evolution does not necessarily occurred in the TRAPPIST-1 planetary system.

A similar study was performed also by Dencs & Regály (2019). These authors studied the amount of water delivered to the planets from a water-rich asteroid belt located just beyond the snow line, and also found that this is a plausible way to deliver the water to the planets. However, Dencs & Regály (2019) assumed a presence of an additional planet in the TRAPPIST-1 system, embedded in the asteroid belt. Although the existence of such a planet in the system cannot be ruled out, it is not discovered so far.

In more broader context, the dynamics of stellar encounters (Jiménez-Torres et al. 2013; Feng & Bailer-Jones 2013) can affect the orbital motion of planetesimals, in particular those coming from the outer parts of a planetary system. Both, systematic tidal effects of the Galactic disk, and stochastic effects of encounters with spiral arms, giant molecular clouds, supernova remnants, etc. represent major influences on habitability of planets within individual planetary systems. This highlights the importance of galactic environment for the habitability studies of the individual planetary systems. In turn, this means that the results of the above described, and similar works (including the one presented in this paper), are also relevant for considering the Milky Way habitability timescales, such as in Došović, Vukotić, & Čirković (2019).

In this work we have searched for an alternative scenario that would explain water delivery to the planets in TRAPPIST-1 system. We have studied a long term dynamical evolution of an asteroid-like planetesimal belt within the currently proposed architectures of the system, and considered a potential amount of water delivered from the belt.

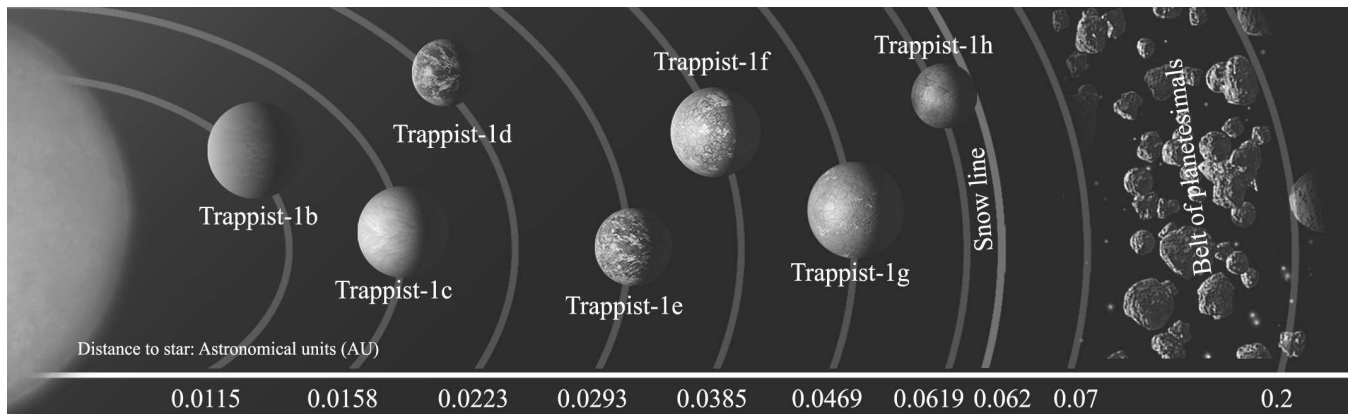


Figure 1. Sketch of the TRAPPIST-1 system with seven planets. In addition to the planets, our hypothetical planetesimal belt and the location of the snow line (light blue) are shown. Credit: adapted from NASA/JPL-Caltech.

2 NUMERICAL SIMULATIONS

2.1 Numerical integrations

In order to analyze a long-term dynamical evolution of planetesimals in the TRAPPIST-1 system, we used numerical simulations.

Observational data suggest that warm planetesimal belts often form in neighborhood of a snow line (Martin & Livio 2012). As our goal is to simulate evolution of the hypothetical asteroid-like planetesimal belt, we assume that its inner edge approximately corresponds to the location of the snow line in the TRAPPIST-1 system. The radial extension of this belt is assumed to correspond to the extension of the asteroid belt in Solar system, but scaled to the size of the TRAPPIST-1 system.

Location of the snow line in the TRAPPIST-1 system is determined using methodology described in Ogihara & Ida (2009) for optically thin disk. Based on their paper, we found that the snow line should be located at 0.062 au, just beyond the outermost planet Trappist-1h (see Fig. 1). Moreover, scaling from the size of the Solar System asteroid belt, we estimated that the planetesimal belt should extend till 0.2 au. We would like to note here that without an extra planet outside 0.2 au in the TRAPPIST-1 system, the disk of planetesimals could in principle spread beyond this limit. However, as results of our simulations presented in Section 3 show, the planetary perturbations at this location should be negligible, and therefore, this unused part would not contribute anyhow to the amount of water delivered to the planets.

Orbital elements of test particles are distributed according to expected structure of a somewhat excited protoplanetary disc (Armitage 2010). The particles are uniformly distributed in terms of orbital semi-major axis, from 0.07 to 0.2 au, and in terms of orbital eccentricity, from 0.0 to 0.2. A half-normal distribution is adopted for the orbital inclinations, above the mid-plane of the protoplanetary disc, with a standard deviation of 1° . The remaining three angular orbital elements are distributed randomly from 0 to 360° . All distributions are produced using generators from NUMPY package.

The simulations are performed using a public domain

MERCURY¹ software package (Chambers 1999). This package has been widely used to simulate dynamics of planetary systems (e.g. Morbidelli 2002; Veras & Ford 2009; Gajdoš et al. 2019). Indeed, Wisdom (2017) recently pointed out that some parts of *Mercury* code may not be properly described in Chambers (1999), but nevertheless, Rein et al. (2019) showed that this has no influence on accuracy and performance of the integrators.

For the purpose of this study, we used two different integrators from the MERCURY package. The most of the simulations are performed using *mixed-variable symplectic* (MVS) integrator (Wisdom & Holman 1991), but in order to have more reliable results, a subset of orbits of planetary-approaching planetesimals are numerically propagated using also *hybrid* integrator (Chambers 1999).

Numerical integrations of the TRAPPIST-1 system are performed using the dynamical models that include seven planets as massive objects, and 20000 planetesimals as massless test particles. In order to investigate how sensitive is the transport of water to the planets on the dynamical model, we use two different models of the TRAPPIST-1 system available in the literature (Wang et al. 2017; Grimm et al. 2018). From these models we adopted the initial conditions for planets, including their orbital elements as well as physical characteristics such as masses and radii (see Table 1).

The time span of numerical integrations is determined using a time scale in the Solar System which is in most cases long enough to trace dynamical evolution of small bodies. This time scale was found to be around 10 Myr (see e.g. Knežević & Milani 2003). As the relevant time scale corresponds to a number of orbital periods, we found that a typical period of an asteroid in the Solar system asteroid belt is about 20 times longer than a period of an object from our assumed planetesimal belt. Therefore, in the numerical simulations of the TRAPPIST-1 system we have propagated the orbits over a time span of 0.5 Myr.

As already mentioned above, the orbits of 20000 planetesimals are initially propagated using the MVS integrator, and their orbital elements are sampled every 50 yr. These

¹ The package is written in FORTRAN 77, and is available at <https://github.com/4xxi/mercury>.

Table 1. The initial orbits and masses for planets in TRAPPIST-1 system, from two different models. In the table, letter G refers to model of [Grimm et al. \(2018\)](#), and letter W refers to model of [Wang et al. \(2017\)](#)

Planet Model	^b		^c		^d		^e		^f		^g		^h	
	W	G	W	G	W	G	W	G	W	G	W	G	W	G
Mass [M_\oplus]	0.790	1.017	1.630	1.156	0.330	0.297	0.240	0.772	0.360	0.934	0.566	1.148	0.086	0.331
Planetary radius [R_\oplus]	1.086	1.121	1.056	1.095	0.772	0.784	0.918	0.910	1.045	1.046	1.127	1.148	0.715	0.773
Semi-major axis [au]	0.01111	0.01155	0.01522	0.01582	0.02145	0.02228	0.02818	0.02928	0.03710	0.03853	0.04510	0.04688	0.05960	0.06193
Eccentricity	0.019	0.006	0.014	0.007	0.003	0.008	0.007	0.005	0.011	0.010	0.003	0.002	0.086	0.006
Inclination [°]	89.393	90.000	89.626	90.000	89.866	90.000	89.754	90.000	89.694	90.000	89.707	90.000	89.814	90.000
Longitude of ascending node [°]	307.0	0.0	201.5	0.0	338.7	0.0	322.2	0.0	199.2	0.0	190.4	0.0	269.9	0.0
Longitude of pericenter [°]	0.0	336.9	40.0	282.5	80.0	-8.7	110.0	108.4	160.0	368.8	195.0	191.3	230.0	338.9
Mean anomaly [°]	344.0	203.1	232.9	69.9	371.0	173.9	185.5	347.9	4.5	113.6	185.9	265.1	93.2	269.7

results are then analyzed for potential close encounters between planetesimals and planets. The particles that passed at a distance smaller than $0.1R_H$ (where R_H is a Hill's radius of a corresponding planet)² from any of the planets, as well as those whose perihelion distance at any time of the integration was smaller than the aphelion distance of the most distant planet in the system, namely Trappist-1h, are identified and their orbits are propagated again. These second integrations are performed using the hybrid integrator with an adaptive time-step, and two sets of outputs are recorded: the orbital elements of planetesimals, and the parameters of close approaches. Since during a single close encounter, any planetesimal could, in principle, pass several times inside the 0.1 Hill's radius of the planet, only the data on the closest approach is kept.

2.2 Mass of the planetesimal belt

The above adopted number of 20000 planetesimals is an arbitrary number selected to be large enough for statistical purposes, but also small enough to avoid highly time-consuming simulations. It is however very important to estimate a realistic number of objects expected in a belt similar to the planetesimal belt assumed in this work.

In order to find a mass of the planetesimal belt, we need to find mass of the whole protoplanetary disc. For this purpose, we assumed that mass of the disk M_{disk} represents 1% of the mass of the host star M_* , i.e. $M_{\text{disk}} = 0.01M_*$, and dust to gas ratio in the disk of $f = 0.01$ ([Armitage 2010](#)), is adopted. Based on this, we estimated a total mass of solids in the disk to be $M_{\text{solid}} = 10^{-2}M_{\text{disk}} = 10^{-4}M_*$.

Using the mass of solids in the disk, adopting a surface density profile in the form

$$\Sigma = \Sigma_0 r^{-\beta}, \quad (1)$$

and assuming an exponent $\beta = 1.5$, as in the Solar System ([Weidenschilling 1977](#)), the mass of the planetesimal belt M_{belt} could be determined by integrating the above equation from the inner to the outer edge of the belt. This yields the following expression:

$$M_{\text{belt}} = M_{\text{solid}} \frac{\frac{1}{r_1^{0.5}} - \frac{1}{r_2^{0.5}}}{\frac{1}{a_1^{0.5}} - \frac{1}{a_2^{0.5}}}, \quad (2)$$

² Due to numerous close encounters in the system, recording these encounters is highly memory demanding. In this respect, our choice to consider only encounters within $0.1R_H$ is found to provide a good compromise between accuracy and resource consumption.

where r_1 and r_2 are inner and outer bounds of the planetesimal belt, respectively, while a_1 and a_2 represent borders of the whole Trappist-1 protoplanetary disc, adopted to be 0.01 and 200 au, respectively.

The inner border of protoplanetary disc is taken to be inside the orbit of the innermost planet Trappist-1b. The value of the outer border is selected based on protoplanetary disc models and observations ([van der Marel et al. 2013](#)), and is large enough to ensure that only negligible mass fraction of the disk may be found outside this limit. With these assumptions, we estimated the mass of the planetesimal belt to be $M_{\text{belt}} = 0.46 M_\oplus$, assuming that whole mass of solids available in this part of the disk is incorporated into the planetesimals.

The study of [Raymond, Quinn & Lunine \(2005\)](#) could be interpreted as suggesting a somewhat higher value of β in the TRAPPIST-1 system, as compared to the Solar System one, since they find steeper density profiles correlated with more terrestrial planets present in simulations. In the same time, however, this would make the uncertainty in position of the outer edge of the planetesimal belt less important, since outermost parts would negligibly contribute to the total mass. However, we decided to use the same value as in Solar System for parameter β . With some other value for β we would get different estimation for mass of planetesimal belt, thus only the scaling factor from number of test particles to the real number of planetesimals would be different.

The next step is to determine a size-frequency distribution (SFD) of planetesimals. The SFD of small objects in a planetary system are usually assumed to be in a form

$$N(> D) = N_t D^{-\alpha}, \quad (3)$$

where N_t is the total number of objects and D is given in kilometers. Therefore, in order to determine the SFD of objects in the planetesimal belt (under the assumption that there is no preferential selection by size), we should know the parameter α .

[Tsirvoulis et al. \(2018\)](#) found that the exponent α of primordial cumulative size distribution of objects in the Solar System asteroid belt should be $\alpha = 1.43$, for objects below 100 km in diameter, and $\alpha = 2.5$ for objects larger than 100 km in diameter.

If we assume that all test particles are spherical, total mass in planetesimal belt M_{belt} could be expressed as:

$$M_{\text{belt}} = \frac{1}{6}\rho\pi \sum_{i=1}^{N_t} D_i^3, \quad (4)$$

where ρ represents density of planetesimals, N_t total number of planetesimals in our model and D_i diameter of i -th

planetesimal. For the density of planetesimals we assume 2 g/cm^3 , similar to the density of water-bearing asteroid (1) Ceres (Park et al. 2016).

Combining the above-given Equations 3 and 4, and assuming that all the mass is concentrated in objects larger than 17 km in diameter, the mass of the planetesimal belt could be expressed as a function of total number of planetesimals in a form:

$$M_{\text{belt}} = \frac{1}{6} \rho \pi \sum_{N=1}^{N_t} \left(\frac{N}{N_t} \right)^{-3/\alpha}. \quad (5)$$

Denoting with $[A]$ the largest integer number smaller than a real number A , and substituting $[N_t \cdot 100^{-1.43}]$ with N_B , we could write:

$$M_{\text{belt}} = \frac{1}{6} \rho \pi \left[\sum_{N=N_B+1}^{N_t} \left(\frac{N}{N_t} \right)^{-\frac{3}{1.43}} + \sum_{N=1}^{N_B} \left(\frac{N}{N_t \cdot 100^{-\frac{2.5}{1.43}}} \right)^{-\frac{3}{2.5}} \right]. \quad (6)$$

Solving the last equation iteratively, we found that there should be more than 2.84 million planetesimals in the belt around TRAPPIST-1 star. Numerical simulation of dynamical evolution with this number of objects would be computationally very demanding. Therefore, we decided to work with 20000 test particles, and then to linearly scale all the obtained results so that they correspond to the estimated number of objects.

3 RESULTS AND DISCUSSION

The numerical simulations described above are performed in order to analyze dynamical evolution of the planetesimal belt in TRAPPIST-1 system, focusing primarily on the influence of the planetesimals on the planets. In this respect, we studied source regions of potential impactors, determined the impact rate and its evolution over time, and estimated the total amount of water that could be potentially delivered to each planet.

As mentioned in Section 2.1, we run the simulations for two different sets of initial conditions taken from Grimm et al. (2018) and Wang et al. (2017). One of the key differences between these two sets are in masses of the planets, with the masses from Grimm et al. (2018) being mostly larger than those from Wang et al. (2017). This is particularly the case for the outermost planet 1h (see Table 1). The results of this work mostly rely on the simulations with the initial conditions from Grimm et al. (2018). However, we have also presented the results of the simulations initiated with the values from Wang et al. (2017), in order to get a better insight into the robustness of the results.

3.1 Dynamical evolution of the planetesimal belt

The first step was to extract from 20000 test particles only those that have close approach with at least one of the planets. In the first set of simulations³, performed using MVS integrator, we found 1726 (about 8.6%) and 1709 (about 8.5%)

of such particles, using the model of Grimm et al. (2018) and Wang et al. (2017), respectively. Very similar numbers obtained with two different models might be a hint that results are not highly model sensitive.

Fig. 2 shows the snapshots from the simulations of the dynamical evolution of the planetesimal belt within both models. The figure reveals that the most perturbed planetesimals during the dynamical evolution follow the line at which the planetesimals' periastron distance is equal to the apoastron distance of the planet Trappist-1h. The objects that reach this line become unstable due to repeated close encounters with planet 1h, and consequently leave the system quickly. We underline also that the most strongly perturbed planetesimals are located close to the inner border of the belt, while beyond about 0.1 au perturbations practically vanish. General behaviors are very similar in both dynamical models. It should be however noted (see two bottom panels in Fig. 2) that after 0.5 Myr of the evolution practically there are no planetesimals intersecting the orbit of the outermost planet 1h in the model of Grimm et al. (2018), while there is still non-negligible fraction of such objects visible in the simulation based on the model of Wang et al. (2017). We believe this is a consequence of significantly larger mass of Trappist-1h in the model of Grimm and coauthors.

Among the objects that have been removed before the simulation ends after 0.5 Myr, 13% are ejected from the TRAPPIST-1 system, 8% collide with the central star, while remaining 79% impact the planets. If we exclude planetesimals whose orbits initially intersect the orbit of the Trappist-1h, the numbers are somewhat different. In this case only 4% are ejected, 2% collide with the central star, and 94% of planetesimals impact the planets.

The further investigations are performed using the second set of the simulations, that is produced using only 1726 (1709) objects that had close approaches with the planets in the first set of the simulations. Their orbits are propagated again for 0.5 Myr, with the same initial conditions as for the first set, but using the hybrid integrator with an adaptive time step.

The results from the second set of integrations, presenting a number of impacts as a function of the distance from the host star, are shown in Fig. 3. These results immediately point out the source region in terms of the initial orbital semi-major axis, from which potential impactors are dominantly originating. It could be easily seen in Fig. 3 that almost all potential impactors are coming from the inner boundary of the planetesimal belt, irrespective of the selected set of the planetary initial conditions. Some of the impactors were initially placed on the orbits that intersect orbit of planet Trappist-1h, making therefore their dynamical evolution controlled by direct gravitational interaction with this planet. Close approaches with the planet 1h quickly increase orbital eccentricity of these particles, putting them on the orbits that intersect the orbits of the other planets as well.

Relative velocities at the time of close encounters may provide useful information about impact conditions. Distribution of relative velocities with planets from the TRAPPIST-1 system are shown in Fig. 4. Since this system is very compact, orbital velocities of the planets are very high, and for the closest planet 1b, this velocity is about 80 km/s. When combined with not so small orbital eccen-

³ First set of simulations was performed using 200 batches with 100 test particles each, i.e. 20000 particles in total.

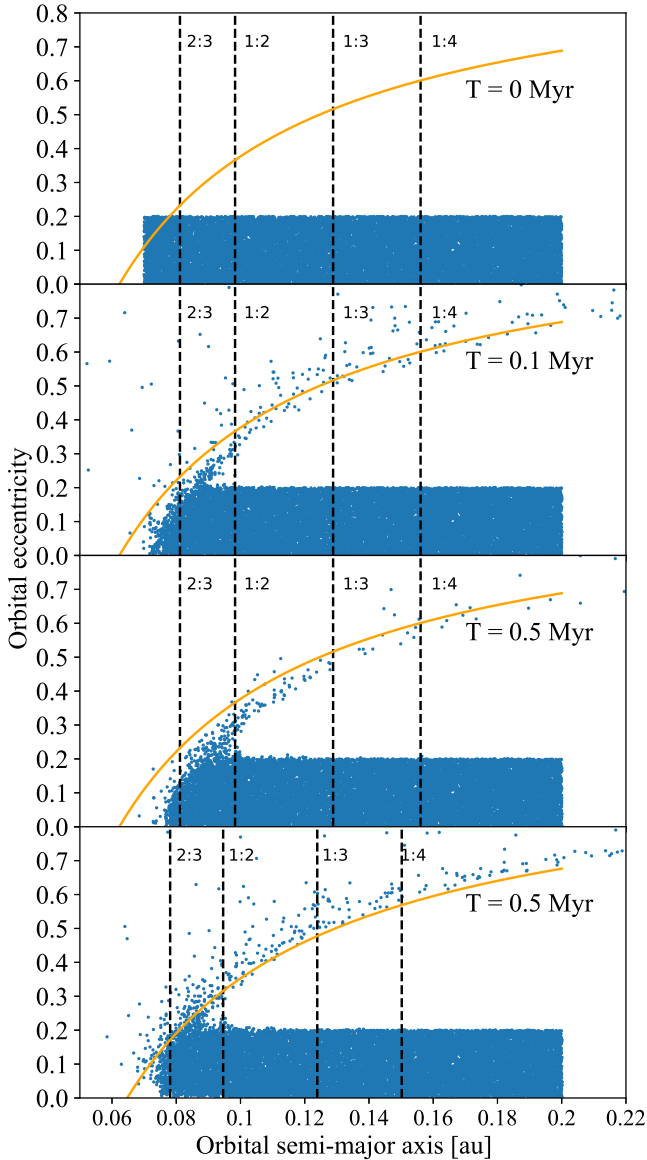


Figure 2. Snapshots from the dynamical evolution of the planetesimal belt. Figure shows evolution of 20000 test particles in the $a-e$ plane. The upper three panels show evolution within the model of [Grimm et al. \(2018\)](#), at the beginning of the simulation (topmost panel), after 0.1 Myr years (second panel), and after 0.5 Myr (third panel from above). The lowermost panel presents the evolution after 0.5 Myr of integration obtained with the model of [Wang et al. \(2017\)](#). Orange line marks location where the periastron distance of planetesimals is equal to the apoastron distance of the planet Trappist-1h. Black dashed line shows positions of the strongest mean-motion resonances with the most distant planet in the system, Trappist-1h.

tricies of planetesimals that may impact the planets, this results in a very high relative velocities.

Distribution of relative velocities with planet 1b exhibits a single peak at about 30 km/s (Fig. 4). It is useful to note here that [Kral et al. \(2018\)](#) performed similar study, but assuming more distant planetesimal belt with very eccentric trajectories, similar to the orbits of Long Period Comets in Solar System. In their analysis of relative velocities, however, Kral and coauthors found two peaks (Figure 6 in [Kral et al. 2018](#)). This fact is a consequence of different

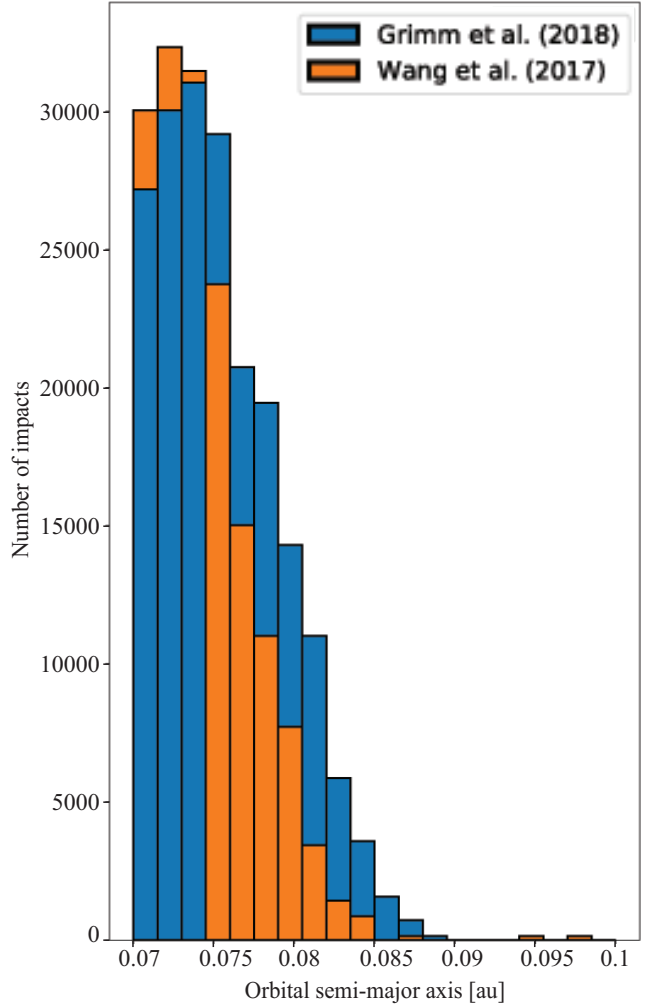


Figure 3. Number of objects impacting the planets in the TRAPPIST 1 system, as a function of their initial semi-major axis, for the two different sets of initial conditions (see legend). Note that the results are scaled to the expected real number of planetesimals in the TRAPPIST-1 system. Both distributions peak close to the inner edge of the planetesimal belt.

orbital eccentricities of planetesimals assumed by [Kral et al. \(2018\)](#) and in this work.

A number of impacts on planets over the 0.5 Myr long time interval is given in Fig. 5. From this figure, a trend of exponential decay of the number of close approaches over time can be noticed. This indicates rapid depletion of the source regions of potential impactors. Fig. 5 also shows a total number of impactors with individual planets. The distributions of impacts on different planets obtained for two models are significantly different, as can be seen from this figure. In the model of [Wang et al. \(2017\)](#), planet Trappist-1b receives cumulatively by far the most of the impacts, while the rest of the planets are significantly less frequently impacted. On the other hand, in the model of [Grimm et al. \(2018\)](#) planets receive relatively similar number of impacts, with the two innermost planets being somewhat less frequently impacted.

In order to investigate in more details how flux of planetesimals towards each of the planets fades over time, we

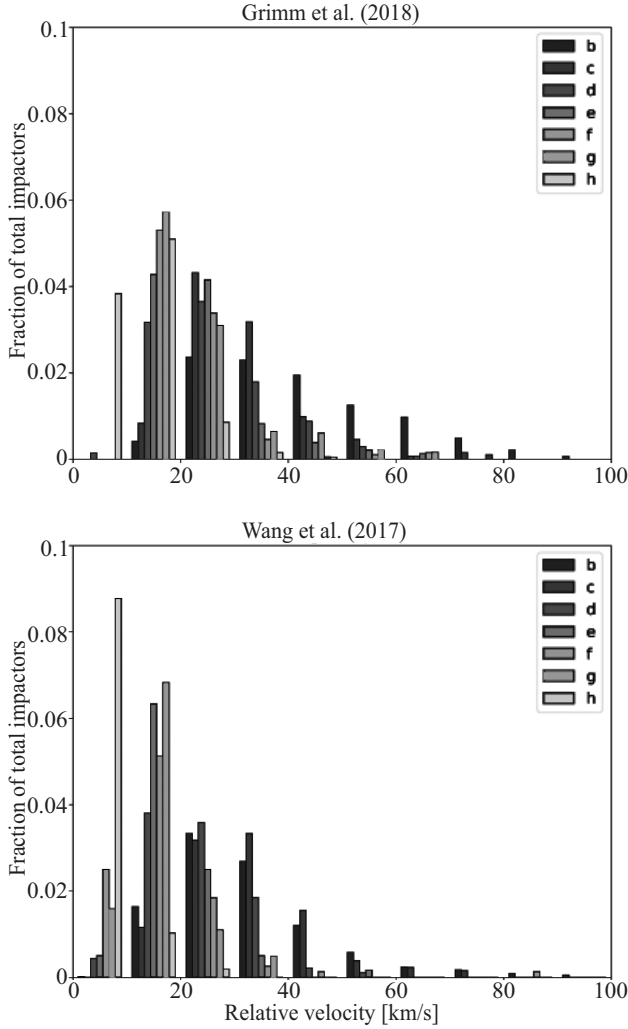


Figure 4. Histogram of relative velocities between planetesimals and planets in TRAPPIST-1 system, at the moments of impacts. The upper panel shows results for [Grimm et al. \(2018\)](#) model, while the lower panel presents results obtained using [Wang et al. \(2017\)](#) model. Each planet is presented with different colour (see legend). Two panels correspond to the two labeled models.

determine the so-called dynamical *half-life*⁴ of impactor population. To this purpose the results shown in Fig. 5 are fitted with a function of the form

$$N(t) = N_0 \cdot e^{-\frac{\ln 2}{\tau} t} \quad (7)$$

(e.g. [Wood et al. 2018](#)), where N is a number of impactors at an arbitrary time t , N_0 is an initial number of impactors, and τ is a half-life.

The obtained results are given in Table 2. It is immediately clear that dynamical lifetime of impactors is very short, with the half-lives for [Grimm et al. \(2018\)](#) model decreasing from about 207 kyr for the innermost planet 1b, to only about 146 kyr for the outermost planet 1h. For [Wang et al. \(2017\)](#) model we found somewhat longer lifetimes of impactor populations, but still shorter than 1 Myr (see Table 2). Therefore, source regions of impactors will be almost completely depleted on the timescale shorter than 1 Myr.

⁴ *Half-life* is the time required for a given population to decrease to half its initial value.

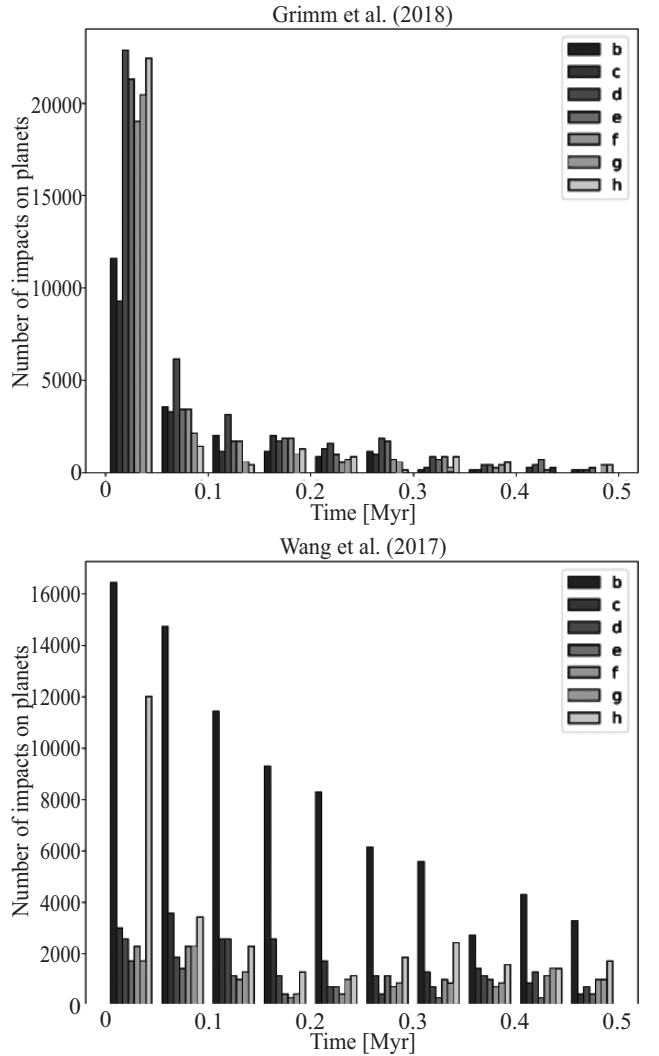


Figure 5. Time distribution of the number of planetesimal impacts to the planets in the TRAPPIST-1 system. Two panels correspond to the two labeled models.

This suggests that impacts on the planets in TRAPPIST-1 system from the planetesimal belt located near the snow line are possible only for a short period of time in comparison to the age of the system. These dynamical half-life times also imply planetesimals transportation time scale of ≈ 50 kyr. This implies that the compact planetary systems, such as TRAPPIST-1 can incorporate material from their outskirts to the innermost planets in a relatively very short time interval.

The source region of potential impactors is crossed by one mean-motion resonance of the first order, namely 2:3 with Trappist-1h. This resonance is located at semi-major axis of 0.0812 au, and may play an important role in the transport of material from the belt to the planets. The mechanism at work here is similar as in the case of the 3:1 mean-motion resonance with Jupiter in the Solar System ([Gladman, et al. 1997](#)). The 2:3 resonances with the planet 1h increases the orbital eccentricity of affected objects till their periastron distance become small enough to allow close encounters with the outermost planet 1h. Once this happens, the close encounters take the leading role in

Table 2. Dynamical half-lives of impactors for each planet in the TRAPPIST-1 system, and from two different dynamical models of the system.

Planet	Dynamical half-life [kyr]	
	Grimm et al. (2018)	Wang et al. (2017)
Trappist-1b	207	378
Trappist-1c	191	425
Trappist-1d	183	447
Trappist-1e	166	462
Trappist-1f	161	458
Trappist-1g	151	853
Trappist-1h	146	143

transporting these objects towards the inner part of the system.

In order to maintain a flux of planetesimals towards the planets in the TRAPPIST-1 system over longer timescales, an additional mechanism that would inject new planetesimals in the unstable regions is needed. In the Solar system, for km-sized objects, this role is played by the non-gravitational Yarkovsky effect (Bottke, Vokrouhlický, Rubincam & Nesvorný 2006). This effect changes the orbital semi-major axis of minor bodies, allowing many of them to reach the resonances.

In order to estimate importance of the Yarkovsky effect in the TRAPPIST-1 system, we used a model of Vokrouhlický (1998, 1999), and estimated that for objects of 1 km in size an expected semi-major axis drift rate is about $da/dt = 1.5 \times 10^{-6}$ au/Myr. This value is about three orders of magnitude smaller than those obtained for the asteroid belt in the Solar system (Vokrouhlický, Bottke, Chesley, Scheeres & Statler 2015; Novaković, Tsirvoulis, Granvik & Todović 2017), which is due to a low luminosity of the Trappist-1 star compared to Solar luminosity. Therefore, the Yarkovsky effect seems negligible in the TRAPPIST-1 system, and consequently an initial flux of planetesimals from the identified source regions should decay very quickly, and should practically vanish in less than 1 Myr. However, it should be noted that due to the compactness of the system, objects need to cross comparatively smaller distance in order to reach unstable regions. Therefore, the Yarkovsky effect might still be relevant for sub-kilometer bodies.

3.2 Alternative source regions

As discussed above, the mean-motion resonance 2:3 with Trappist-1h is located inside the main source region of potential impactors, and may significantly influence dynamical evolution of the planetesimal belt. Therefore, although a Jupiter-mass planet⁵ has not been discovered in the system (Gillon et al. 2017), neither it is expected to exist (Boss, et al. 2017), we found that first-order mean-motion resonance with a sub-Earth-mass planet are powerful enough to induce strong orbital perturbations.

In order to understand better a potential role of other mean-motion resonances, here we explore the effect of another first-order mean-motion resonance in the system, namely the 1:2 resonance with Trappist-1h.

We note here however that this resonance is located at about 0.0983 au, and that we did not see any obvious effect at this location in our numerical simulations (see Fig. 2). Nevertheless, we decided to investigate the role of the 1:2 resonance in detail. For this purpose, we adopted an approach developed by Novaković, Tsiganis, & Knežević (2010) to study diffusion among asteroid families.⁶

The diffusion is measured in space of two actions defined as $J_1 \sim 1/2\sqrt{a/a_p}e^2$ and $J_2 \sim 1/2\sqrt{a/a_p}\sin^2(i)$ (Novaković, Tsiganis, & Knežević 2010), where a , e and i are semi-major axis, eccentricity and inclination respectively, while index p is used to denote orbital elements of the planet, in this case 1h. Hence, we generate a new set of 100 test objects located inside the 1:2 resonance, and propagate numerically their orbits for 10 Myr, using the dynamical model from Grimm et al. (2018). From these data we have produced a time-series of J_i . Finally, we assume a linear diffusion, and the so-called diffusion coefficients $D(J_i)$ are obtained by linear fitting of time series of $\langle(\Delta J_i)^2\rangle$, ($i = 1, 2$), determined from the numerical integration for each action J_i .

The obtained results reveal that the orbit diffusion process inside this resonance is slow, but non-negligible. A significant change in J_1 occur on time scale ~ 1 Gyr (Figs. 6). In other words, objects initially placed on eccentric orbits ($e \geq 0.2$) may evolve to the planet Trappist-1h crossing-orbit on the time scale of about 1 Gyr. As shown in Fig. 7, diffusion is about an order of magnitude slower in J_2 action. Nevertheless, the diffusion observed in the J_1 action suggests that the 1:2 mean-motion resonance might be a source of additional impactors after initial phase of evolution of the belt, which takes 1 Gyr. Once the resonance remove all planetesimals trapped inside it, additional particles could be inserted by collisions near the borders of the resonance (Zappalà, et al. 1998), thus producing a new flux towards the planets, but of generally smaller objects.

3.3 Water transport to the planets

An important step in our analysis is to determine the amount of water transported to the planets by planetesimals. To this purpose we used close encounters data presented in Section 3.1. Specifically, if a distance between a planetesimal and a planet is found to be smaller than the radius of the planet (see Table 1), we assume that an impact occurs. Next, we also assume that each planetesimal has a water content of 5% by volume, and that during the impacts planetesimals transfer the whole amount of water to the planets, i.e. do not account for the potential water loss that could occur during accretion (O’Brien et al. 2014; Ciesla, et al. 2015).

The amount of water delivered to each planet is expressed as percentage of the Earth’s water amount (here-

⁵ Formation of a big Jupiter-mass planets around M dwarf stars is generally unlikely (Laughlin, Bodenheimer & Adams 2004)

⁶ Asteroid families are populations of asteroids that have very similar orbits, and are thought to be fragments of past asteroid collisions (Milani, et al. 2014).

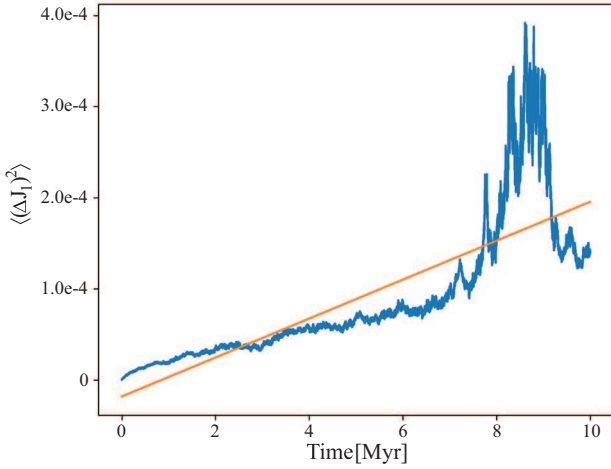


Figure 6. Time evolution of mean-square displacement in J_1 action for objects inside the 1:2 mean motion resonance with Trappist-1h (blue curve), and its corresponding linear fit (orange line).

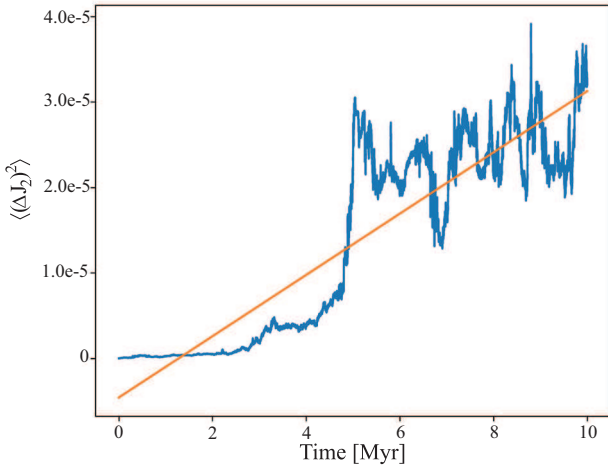


Figure 7. Same as on Fig. 6, but for action J_2 .

after EWA). In this respect, let us recall that the amount of Earth’s water in all aggregates is estimated to be $1,386,000,000 \text{ km}^3$ (Peter H. Gleick 1993).

The cumulative amount of water delivered to the planets is shown in Fig. 8. The results obtained using the dynamical model by Grimm et al. (2018) suggest that the largest amount of water could be delivered to the planets 1e and 1g. Each of these two planets received more than 65% of EWA. However, it is even more important to note in these results that practically all the planets received non-negligible amount of water, with the smallest amount of about 20% of the EWA being delivered to the planet 1b (see top panel in Fig. 8). Excluding planetesimals that initially cross the orbit of Trappist-1h reduces slightly the amount of water delivered on the planets (bottom panel in Fig. 8). Still, the main conclusions remain the same, and the delivered amount of water is in excess of 15% of the EWA for all the planets.

The results are different in the simulations performed with the initial conditions suggested by Wang et al. (2017). In this case, the largest amount of water is delivered to the planets 1b, 1g and 1h, in each case more than 50% of Earth’s water content, while the planets 1c and 1e received

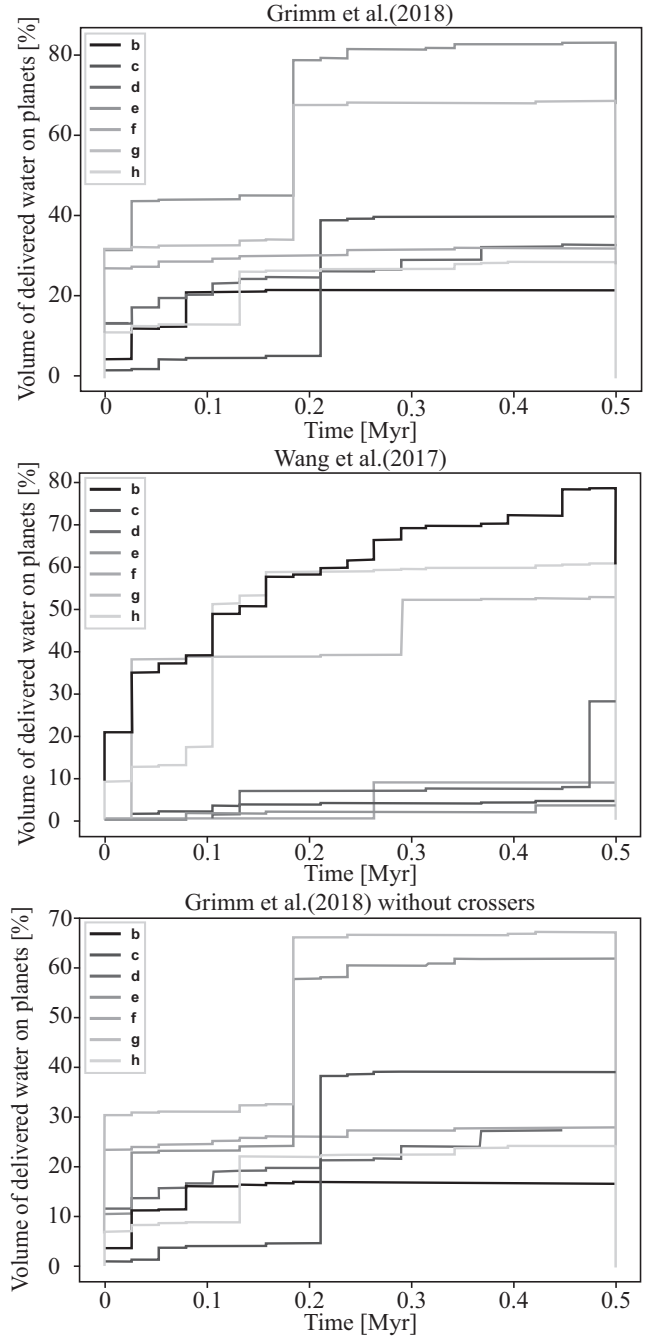


Figure 8. Cumulative amount of water delivered to planets as a function of time, expressed as a fraction of the Earth’s water volume. The results for model of Grimm et al. (2018) are shown in the upper panel, while model of Wang et al. (2017) is shown in the middle panel. The lower panel shows the model of Grimm et al. (2018), with the intersecting planetesimals excluded. Note that larger jumps in the amount of delivered water are associated to the impacts of big planetesimals. As the amount is estimated by scaling from the number of the simulated particles to the real number of objects in planetesimal belt, the timeline of water delivery may not be fully certain, but still the total amount should be realistic.

only a few percents of the EWA. Therefore, although generally transport of significant amount of water to the planets in TRAPPIST-1 system via planetesimals is definitely possible, the results are model dependent to some extent. It should be noted, however, that Trappist-1b is very close to the host star, and therefore it is expected that any water delivered to this planet may exist only in gaseous state. On the other hand, in the case of Trappist-1h, it is expected that water delivered on this planet is frozen. The planet that receives more than 50% of EWA, regardless of the applied set of initial conditions, is 1g. Interestingly, this is one of three planets located inside the habitable zone, (Papaloizou, Szuszkiewicz, & Terquem 2018), thus it is possible that at least some of its water may be in liquid state.

Recently several works performed composition and climate modeling of planets in the TRAPPIST-1 system. Grimm et al. (2018) have analyzed the nature of planets in TRAPPIST-1 system, and obtained so far the most precise densities of these planets. Regarding the composition, their results could be summarized in the following. The planets 1c and 1e are likely rocky, while the planets 1b, 1d, 1f, 1g, and 1h may have envelopes of volatiles in the form of thick atmospheres, oceans, or ice. Especially, these authors found that planets 1b, 1d, and 1g almost certainly are volatile-rich. More recently, Unterborn, Hinkel & Desch (2018) performed more detail modeling of planetary composition in TRAPPIST-1 system and obtained results generally consistent with that of Grimm et al. (2018). In particular, Unterborn, Hinkel & Desch (2018) found that for planets 1b, 1d, and 1f, the results strongly suggest the presence of planetary surface volatiles, but pointed out that the results are model dependent, and more refined mass and radius measurements of the TRAPPIST-1 planets are needed for better characterization.

Some climate models of TRAPPIST-1 planets suggest that Trappist-1e, if it is today in synchronous rotation state and abundant in water, then this planet should always sustain surface liquid water at least in the sub-stellar region, whatever the atmosphere considered (Turbet, et al. 2018). Also, Lincowski et al. (2018) suggest that Trappist-1e may produce habitable surface temperatures beyond the maximum greenhouse distance.

It is interesting to compare our results with predictions based on the above-mentioned climate and composition models of planets in the TRAPPIST-1 system. In this respect, these models all predict that planet 1f should contain a significant amount of water. The results of our simulations performed within the dynamical model from Grimm et al. (2018) are in reasonably good agreement with the prediction by the climate and composition models, except maybe for planet 1b. However, the results obtained using Wang et al. (2017) model predict only a small amount of water may be delivered to the planet 1f via planetesimals. For planet 1g, within the both dynamical models we found that this planet should be water-rich, in accordance with the results reported by Grimm et al. (2018) and Unterborn, Hinkel & Desch (2018). The planet 1e is an interesting case. In our model with the initial conditions from Grimm et al. (2018) this planet receives a huge amount of water. This result is in disagreement with those by Grimm and coauthors, who found that 1e should be dry rocky planet. On the other hand, several other papers

(Lincowski et al. 2018; Turbet, et al. 2018) considered the possibility that the planet 1e may be tidally locked aqua-planet, in agreement with our results, regarding the water content. Still, using the model from Wang et al. (2017), we found that planetesimals could deliver only a very modest amount of water to the planet 1e, but a large amount to 1b. The results for 1e clearly illustrate that the current predictions are still not well constrained, and the situation is generally similar for all the planets. Therefore, further theoretical and observational efforts are needed to improve the models and clarify these issues.

The discriminants between the predicted compositions require additional observational data, and new models that will involve different effects as well as their complex mutual interactions (see e.g. Becker, et al. 2020). Nevertheless, our simulations provide useful constraints on possible water transport within the TRAPPIST-1 system. In general, we believe that the mechanism of water delivery to the planets in TRAPPIST-1 system investigated here is plausible, and it may explain the origin of water in at least some of these planets.

Also, we recall here that the water transport via planetesimal mostly occurs in an early phase of the planetary system, while the climate and composition models refer to present states of the planets. Therefore, these results refer to different points in time, and planets may undergo significant evolution (e.g. water loss) in the meantime. This might be an explanation for some of differences between our results and the climate and composition models predictions. Of course, we cannot enter here the complex issue such is water retention, which may be entirely different on planets around M dwarfs due to tidal locking, and strong XUV flares (Godolt, et al. 2019). In addition, the possibility of water retention should be examined against the long term possibilities of water delivery, including the replenishment of the planetesimal belt population with possible means such as the stellar encounters and other possible effects related to the galactic environment. This is of particular importance for the habitability studies of the planetary systems that have a relatively large estimated ages, such as the TRAPPIST-1.

3.4 Limitations of the water transport model

The model of water transport presented here obviously has some limitations.

It is important to note that the 5% water fraction in planetesimals assumed here is very conservative. It is based on what we see today in carbonaceous chondrites, which are the product of the evolution of their parent bodies that formed from a mix of rock and ice a billions of years ago. Therefore, it is likely that these parent bodies contained significantly larger amount of water (Ciesla, et al. 2015). On the other hand, much longer history of the TRAPPIST-1 system allows for evolutionary processes which have not been noticed or appreciated enough in the Solar system context.

Through analysis of the remains of meteorites, which are believed to be asteroids, in the Solar system, it is concluded that they can have 5 – 20% of water (Burbine et al. 2002). Therefore, the percentage of water in planetesimal volume significantly depends on both, the distance between

these objects and their parent star in the moment of their birth, and on their later evolution.

The most important caveat to this work seems to be the location of the snow line. A fraction of volatile materials in planetesimals obviously depends on the location of the snow line; in our model, shifting this line a bit further from the host star, would imply that many planetesimals located close to the inner border of the belt would have a significantly smaller water content. As argued in this work, that the source region of potential impactors in TRAPPIST-1 is confined in the narrow area, exactly at the inner edge of the planetesimal belt, this may significantly affect the estimation of the amount of water delivered to the planets.

The material evaporation during planetesimal impacts should also be considered. It is inevitable that this sort of impacts, and contacts with planetary atmospheres, would cause a certain amount of material loss (de Niem et al. 2012). For this study, the water transport during the impact is considered to be maximally efficient, which is not the case in reality. The amount of evaporated material at the moment of the impact depends on the impact velocity and the escape velocity from the planet (O’Brien et al. 2014). Based on the impact simulation they conducted, mainly for the Earth and Mars, de Niem et al. (2012) have concluded that about 20% of material is lost at the moment of impact. However, this is not the only issue - another issue is whether some of the matter which is not lost in the sense of being ejected is chemically dissociated. One could have water being vaporized, and while formally not lost in these models, still being thermally or photo-dissociated, with hydrogen being subsequently lost through outgassing at longer timescales (and oxygen retained and bound in minerals).

Dynamical evolution of planetesimal belt would be different if there is another distant planet in TRAPPIST-1 system that is not discovered yet (Dencs & Regály 2019), thus also we would expect more delivered water on planets if that is the case.

The mutual gravitational perturbations between the planetesimals are neglected in our model. However, planetesimals larger than about 500 km in diameter may significantly influence the motion of nearby objects (Delisle & Laskar 2012; Novaković et al. 2015). In this respect, we expect that taking into account these perturbations would somewhat increase the total flux of planetesimals towards the planets, resulting in more efficient water transport.

Finally, the limit of the planetocentric distances of $0.1R_H$, that we considered here, is set somewhat arbitrary. However, as we are primarily interested in a number of planetary impacts, we considered the range around the planets from which many close approaches result in an impact. This could slightly affect our results, as some of the planetesimals passing at larger distances might impact the planets as well. Therefore, for this reason our estimation of the total amount of water delivered to the planets could be slightly underestimated.

4 CONCLUSIONS AND FUTURE WORK

4.1 Conclusions

In this work, we have investigated dynamical evolution of the hypothetical, asteroid-like, planetesimal belt in TRAPPIST-

1 exoplanetary system. In particular, we addressed the role of the planetesimals in the origin of water on planets in this system.

The preceding analysis has led us to the following conclusions:

- There are dynamical mechanisms capable to transport significant amount of material from the inner edge of the planetesimal belt to the planets in TRAPPIST-1 system.
- The obtained results suggest that the amount of water that could be delivered to the planets is significant. For individual planets it vary from 15 to 80% of the Earth’s water content.
- The dynamical half-life of impactor population is short, at best a less than one million years. Therefore, the population of impactors decays quickly, and significant transport of materials, including water transport, is possible only within the first several million years since the formation of the planetesimal belt.
- The 1:2 mean motion resonance with planet Trappist-1h could be an additional source of impactors from the belt. It initiates a slow orbit diffusion that over a time-scale of 1 Gyr may drive trajectories of affected planetesimals to planet-crossing orbits.
- The non-gravitational effects in the TRAPPIST-1 system are negligible, and therefore, there are no other efficient mechanisms to resupply new bodies inside the impactors’ source regions.

4.2 Future work

The questions addressed here should be further investigated in order to test these initial findings, and to address some closely related problems. Let us mention a few of them.

Some parameters adopted in our model are not well-constrained, and it would be therefore useful to test wider parameter space. An example is a protoplanetary disc mass, and the gas to dust ratio in disks. In this work, we assumed that mass of the disk is 1% of the star mass (Armitage 2010), and the gas-to-dust ratio of 100. Still, different estimates could be found in the literature. Andrews et al. (2013) suggested that mass of the disks may be somewhat smaller, in the range of 0.2 – 0.6% of the star mass, while in their study of the TRAPPIST-1 system, Ormel, Liu, & Schoonenberg (2017) suggest the disk mass of 4%.

Our model did not account for possible removal of planetesimals in an early phase of the system evolution, as it may be caused, for instance, by planetary migration (Walsh et al. 2012), and that likely occurred in the TRAPPIST-1 system as well (Coleman, et al. 2019). In this respect, it would be interesting to analyze the amount of material transport assuming the mass of the planetesimal belt proportional to the current mass of the Asteroid Belt in the Solar System (Levison, et al. 2015), that is significantly smaller than the one used in our model presented here.

As we have argued above, the location of the snow line significantly affects the estimation of the amount of water delivered to the planets. Therefore, it would be very interesting in future work to test whether larger amount of water content in icy planetesimals would be able to counterbalance potentially smaller impactor source regions, due to possibly more distant location of the snow line in the system.

The habitability studies of such compact planetary systems of similar age should consider the possibilities of water retention together with the replenishment of the planetesimal belt by mechanisms related to the interaction with the galactic environment. This should be investigated together with the possibility that close stellar flybys might destabilize the orbits of planets or alter the flux of small bodies towards the habitable zone of the planetary system.

Finally, from the astrobiological point of view, some recent works suggest that, despite being located inside the habitable zone (O'Malley-James & Kaltenegger 2017), planets Trappist-1e, Trappist-1f and Trappist-1g may not be good habitats because of the extreme ultraviolet radiation from M dwarf host star (Peacock et al. 2019), as well as destructive atmospheric effects of super-flares (Howard, et al. 2018). Only forthcoming searches for biosignatures, however, coupled with better constraints on the age of TRAPPIST-1, will shed some light on the astrobiological status of this fascinating system.

ACKNOWLEDGEMENTS

The authors would like to thank the referee for the valuable comments which helped to improve the manuscript. We acknowledge financial support from the Ministry of Education, Science and Technological Development of the Republic of Serbia: VD and BN through the project ON176011 "Dynamics and kinematics of celestial bodies and systems", and BV and MMĆ through the project ON176021 "Visible and invisible matter in nearby galaxies: theory and observations".

DATA AVAILABILITY

The data underlying this article will be shared on reasonable request to the corresponding author.

REFERENCES

- Andrews S. M., Rosenfeld K. A., Kraus A. L., Wilner D. J., 2013, *ApJ*, 771, 129
- Armitage P. J., 2010, *Astrophysics of Planet Formation* Cambridge Univ. Press, New York
- Becker J., Gallo E., Hodges-Kluck E., Adams F. C., Barnes R., 2020, *arXiv*, arXiv:2005.01740
- Bolmont E., Selsis F., Owen J. E., Ribas I., Raymond S. N., Leconte J., Gillon M., 2017, *MNRAS*, 464, 3728
- Boss A. P., Weinberger A. J., Keiser S. A., Astraatmadja T. L., Anglada-Escudé G., Thompson I. B., 2017, *AJ*, 154, 103
- Bottke W. F., Vokrouhlický D., Rubincam D. P., Nesvorný D., 2006, *AREPS*, 34, 157
- Burbine H. T., McCoy J. T., Jarosewich E., Sunshine M. J., 2002, *anme*, 27, 9
- Burgasser A. J., Mamajek E. E., 2017, *ApJ*, 845, 110
- Campins H., et al., 2010, *Natur*, 464, 1320
- Castillo-Rogez, J. C., & McCord, T. B. 2010, *Icarus*, 205, 443
- Chambers J. E., 1999, *MNRAS*, 304, 793
- Ciesla F. J., Mulders G. D., Pascucci I., Apai D., 2015, *ApJ*, 804, 9
- Coleman G. A. L., Nelson R. P., Paardekooper S. J., Dreizler S., Giesers B., Anglada-Escudé G., 2017, *MNRAS*, 467, 996
- Coleman G. A. L., Leleu A., Alibert Y., Benz W., 2019, *A&A*, 631, A7
- Cuntz M., Loibnegger B., Dvorak R., 2018, *AJ*, 156, 290
- Delisle J.-B., Laskar J., 2012, *A&A*, 540, A118
- Dencs Z., Regály Z., 2019, *MNRAS*, 487, 2191
- de Niem D., Kürt E., Morbidelli A., Mutschmann U., 2012, *Icar*, 221, 495
- de Wit J., et al., 2016, *Nature*, 537, 69
- Dobos V., Barr A. C., Kiss L. L., 2019, *A&A*, 624, A2
- Došović V., Vukotić B., Čirković M. M., 2019, *A&A*, 625, A98
- Dvorak R., Loibnegger B., Cuntz M., 2020, in *The Trans-Neptunian Solar System*, Edited by Dina Prialnik, Maria Antoinetta Barucci, Leslie Young, 2020, Elsevier (arXiv:1903.06910)
- Feng F., Bailer-Jones C. A. L., 2013, *ApJ*, 768, 152
- Frantseva, K., Mueller, M., Pokorný, P., van der Tak, F. F. S., ten Kate, I. L. 2020, *A&A*, in press
- Fritz J., et al., 2014, *P&SS*, 98, 254
- Gajdoš P., et al., 2019, *MNRAS*, 485, 3580
- Gillon M., et al., 2016, *Natur*, 533, 221
- Gillon M., et al., 2017, *Natur*, 542, 456
- Gladman B. J., et al., 1997, *Sci*, 277, 197
- Grimm S. L., et al., 2018, *A&A*, 613, A68
- Godolt M., Tosi N., Stracke B., Grenfell J. L., Ruedas T., Spohn T., Rauer H., 2019, *A&A*, 625, A12
- Goldreich P., Lithwick Y., Sari R., 2004, *ApJ*, 614, 497
- Gonzalez G., 2005, *OLEB*, 35, 555
- Hamilton V. E., et al., 2019, *NatAs*, 3, 332
- Hsieh H. H., Novaković B., Kim Y., Brasser R., 2018, *AJ*, 155, 96
- Hogerheijde M. R., et al., 2011, *Sci*, 334, 338
- Howard, W. S., et al., 2018, *ApJL*, 860, L30
- Ida S., Yamamura T., Okuzumi S., 2019, *A&A*, 624, A28
- Jewitt D., 2012, *AJ*, 143, 66
- Jiménez-Torres J. J., Pichardo B., Lake G., Segura A., 2013, *As-Bio*, 13, 491
- Kama M., et al., 2016, *A&A*, 592, A83
- Knežević Z., Milani A., 2003, *A&A*, 403, 1165
- Kral Q., Wyatt M. C., Triad A. H. M. J., Marino S., Thébault P., Shorttle O., 2018, *MNRAS*, 479, 2649
- Küppers M., et al., 2014, *Natur*, 505, 525
- Kuiper G. P., 1938, *ApJ*, 88, 472
- Laughlin G., Bodenheimer P., Adams F. C., 2004, *ApJL*, 612, L73
- Levison H. F., Kretke K. A., Walsh K. J., Bottke W. F., 2015, *PNAS*, 112, 14180
- Lincowski A. P., Meadows V. S., Crisp D., Robinson T. D., Luger R., Lustig-Yaeger J., Arney G. N., 2018, *ApJ*, 867, 76
- Luger R., et al., 2017, *NatAs*, 1, 0129
- Martin R. G., Livio M., 2012, *MNRAS*, 425, L6
- Martin R. G., Livio M., 2013, *MNRAS*, 428, L11
- McCord T. B., Sotin C., 2005, *JGRE*, 110, E05009
- Milani A., Cellino A., Knežević Z., Novaković B., Spoto F., Paolich P., 2014, *Icar*, 239, 46
- Morbidelli A., 2002, *AREPS*, 30, 89
- Novaković B., Tsiganis K., Knežević Z., 2010, *MNRAS*, 402, 1263
- Novaković B., Maurel C., Tsirvoulis G., Knežević Z., 2015, *ApJL*, 807, L5
- Novaković B., Tsirvoulis G., Granvik M., Todović A., 2017, *AJ*, 153, 266
- O'Brien D. P., Walsh K. J., Morbidelli A., Raymond S. N., Mandell A. M., 2014, *Icar*, 239, 74
- Ogihara M., Ida S., 2009, *AIPC*, 1158, 259
- O'Malley-James J. T., Kaltenegger L., 2017, *MNRAS*, 469, L26
- Ormel C. W., Liu B., Schoonenberg D., 2017, *A&A*, 604, A1
- Papaloizou J. C. B., Szuszkiewicz E., Terquem C., 2018, *MNRAS*, 476, 5032
- Park R. S., et al., 2016, *Natur*, 537, 515
- Peacock S., Barman T., Shkolnik E. L., Hauschildt P. H., Baron E., 2019, *ApJ*, 871, 235
- Peter H. Gleick (editor), 1993, *Water in Crisis: A Guide to the*

- World's Fresh Water Resources (Oxford University Press, New York)
- Pontoppidan K., et al., 2019, BAAS, 51, 229
- Raymond S. N., Quinn T., Lunine J. I., 2004, Icar, 168, 1
- Raymond S. N., Quinn T., Lunine J. I., 2005, ApJ, 632, 670
- Rein H., et al., 2019, MNRAS,
- Rivkin A. S., Emery J. P., 2010, Natur, 464, 1322
- Schoonenberg D., Liu B., Ormel C. W., Dorn C., 2019, A&A, 627, A149
- Snodgrass C., et al., 2017, A&ARv, 25, 5
- Tamayo, D., Rein, H., Petrovich, C., & Murray, N. 2017, ApJ, 840, L19
- Thangjam G., Nathues A., Platz T., Hoffmann M., Cloutis E. A., Mengel K., Izawa M. R. M., Applin D. M., 2018, M&PS, 53, 1961
- Tsiganis K., Gomes R., Morbidelli A., Levison H. F., 2005, Natur, 435, 459
- Tsirvoulis G., Morbidelli A., Delbo M., Tsiganis K., 2018, Icar, 304, 14
- Turbet M., et al., 2018, A&A, 612, A86
- Unterborn C. T., Desch S. J., Hinkel N. R., Lorenzo A., 2018, NatAs, 2, 297
- Unterborn C. T., Hinkel N. R., Desch S. J., 2018, RNAAS, 2, 116
- van der Marel N., et al., 2013, Sci, 340, 1199
- Veras D., Ford E. B., 2009, ApJ, 690, L1
- Vokrouhlický D., 1999, A&A, 344, 362
- Vokrouhlický D., 1998, A&A, 335, 1093
- Vokrouhlický D., Bottke W. F., Chesley S. R., Scheeres D. J., Statler T. S., 2015, Asteroids IV, eds. P. Michel, F. E. DeMeo, & W. F. Bottke, 509
- Walker G., 1995, Natur, 378, 332
- Walsh K. J., Morbidelli A., Raymond S. N., O'Brien D. P., Mandell A. M., 2012, M&PS, 47, 1941
- Wang S., Wu D.-H., Barclay T., Laughlin G. P., 2017, preprint (arXiv:1704.04290)
- Weidenschilling S. J., 1977, Ap&SS, 51, 153
- Westall F., et al., 2015, AsBio, 15, 998
- Wisdom J., Holman M., 1991, AJ, 102, 1528
- Wisdom J., 2017, MNRAS, 464, 2350
- Wolf E. T., Shields A. L., Kopparapu R. K., Haqq-Misra J., Toon O. B., 2017, ApJ, 837, 107
- Wood J., Horner J., Hinse T. C., Marsden S. C., 2018, AJ, 155, 2
- Yang C.-C., Mac Low M.-M., Menou K., 2009, ApJ, 707, 1233
- Zappalà V., Cellino A., Gladman B. J., Manley S., Migliorini F., 1998, Icar, 134, 176